Copper loss analysis based on extremum co-energy principle for high frequency forward transformers with parallel-connected windings

Tomohide Shirakawa, Genki Yamasaki, Kazuhiro Umetani, and Eiji Hiraki
Graduate School of Natural Science and Technology
Okayama University
Okayama, Japan

Published in: IECON 2016 - 42nd Annual Conference of the IEEE Industrial Electronics Society

DOI: 10.1109/IECON.2016.7793013

Copper Loss Analysis Based on Extremum Co-Energy Priciple for High Frequency Forward Transformers with Parallel-Connected Windings

Tomohide Shirakawa, Genki Yamasaki, Kazuhiro Umetani, Eiji Hiraki
Graduate School of Natural Science and Technology
Okayama University
Okayama, Japan
prjo4kx3@s.okayama-u.ac.jp

***Abstract*—The Dowell model is widely utilized for copper loss analysis of forward transformers. However, this model is not directly applicable to transformers with parallel-connected windings. The reason is that the Dowell model requires determining the AC current of all the windings in advance of analysis, although the AC current distribution in parallel-connected windings is severely affected by disposition of the windings. This issue is addressed in this paper by employing the Dowell model in combination with a novel insight that the AC current is distributed in parallel-connected windings to give an extremum of the magnetic co-energy of the transformer. Simulation and experiment were carried out; and, the results supported appropriateness of the proposed copper loss analysis method.**

Keywords—copper loss; transformer; proximity effect; Dowell model; extremum co-energy

I. INTRODUCTION

High frequency forward transformers are commonly utilized in isolated DC-DC converters to generate DC power for low-power consumer appliances from the commercial AC power sources. Because these appliances require power supply with the voltage far smaller than the commercial power source, the forward transformers generally have secondary winding with far fewer number of turns compared with the primary winding. As a result, the large AC current tends to flow in the secondary windings. Therefore, reduction of the copper loss in the secondary winding is intensely required because it can dominate the transformer loss.

Parallel-connected windings can be a useful remedy for the issue because they can increase effective cross-section area for the secondary current [1]–[4]. In many cases, these parallel-connected secondary windings are separately wound on the magnetic core to form their own winding layers; and then, they are connected in parallel at the secondary terminals, for convenient construction of the forward transformers. Typical examples are presented in Fig. 1.

There can be a number of patterns in the disposition of winding layers, as exemplified in Fig. 1. As reported in literature [1], [2], [4], [5], the disposition of winding layers is known to have significant effect on the copper loss. Hence, the disposition of winding layers is one of the important designing points to suppress the copper loss.

A number of techniques have been proposed to elucidate the relation between the disposition and the copper loss. For example, numerical analyses are performed in [2], [4], [5]. Besides, equivalent circuit models of the winding layers are constructed and investigated in [4] and [6]. These techniques are proven to predict the copper loss from the disposition of the winding layers. However, they may suffer from complicated analysis procedure as well as complicated model construction.

For systematical design of the disposition of winding layers, the relation between the disposition and the copper loss should be analyzed preferably using straightforward analytical tools. As a well-known tool, the Dowell model has been widely utilized in transformer design [7]–[14]. The Dowell model can be used to predict the copper loss through analysis of the skin effect and the proximity effect in the windings.

However, the Dowell model requires that the magneto-motive force of all the windings should be given in advance of the analysis [1]. This requirement can cause difficulty in directly applying the Dowell model to transformers with

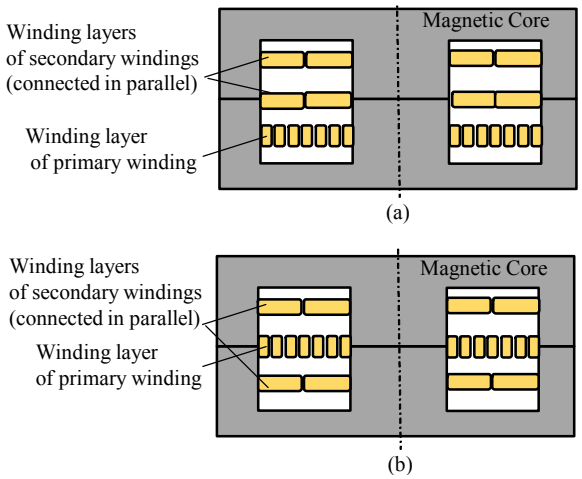

Fig. 1. Two typical examples (a) and (b) of the forward transformers with parallel-connected sedondary windings. (Vertical sectional view)

parallel-connected windings. The reason is that the AC current distribution in these windings may be complicated to predict in many cases, because the AC current distribution depends on the complicated magnetic coupling among the windings, which is severely affected by the physical transformer structure. For example, [1] performed numerical calculation of the 1-dimensional magnetic field analysis to determine the AC current distribution for the Dowell model.

The purpose of this paper is to propose a straightforward analytical method to predict the copper loss in high frequency forward transformers with parallel-connected windings. For convenience, this paper assumes that no DC current flows in the primary and secondary windings, as is usual in practical forward transformers. The proposed method analyzes the copper loss by employing the Dowell model in combination with a novel insight that the AC current is distributed in parallel-connected windings to give an extremum of the magnetic co-energy [15][16] of the transformer. This insight offers straightforward derivation of the AC current distribution in parallel-connected windings. Hereafter, we refer to it as the extremum co-energy principle.

The following discussion consists of 4 sections. Section II presents the extremum co-energy principle. Section III presents the proposed analysis method of the copper loss prediction, as well as some basic examples. Section IV presents experiment that verified the examples. Finally, section V gives conclusions.

II. Extremum Co-Energy Principle

This section demonstrates that the AC current is distributed to give an extremum of the magnetic co-energy of the transformer. This principle neglects the effect of the parasitic resistance of the winding conductor on the current distribution, because the magnetic coupling rather dominates the current distribution in high frequency transformers.

We consider a high frequency transformer with n windings. Let $i_1, i_2, \ldots, i_n$ be the AC current of windings 1, 2, …, n on the transformer, respectively. In addition, let $\psi_1, \psi_2, \ldots, \psi_n$ be the AC flux linkage of windings 1, 2, …, n. For convenience, windings 1, 2, …, k are the primary windings connected in parallel; and windings k+1, k+2, …, n are the secondary windings connected in parallel. Flux linkage $\psi_1, \psi_2, \ldots, \psi_n$ are functions of $i_1, i_2, \ldots, i_n$.

We define the current vector $\mathbf{i}$ as $\mathbf{i} \equiv [i_1, i_2, \ldots, i_n]^t$. In addition, we define a flux linkage vector $\boldsymbol{\psi}$ as $\boldsymbol{\psi} \equiv [\psi_1, \psi_2, \ldots, \psi_n]^t$. Then, the magnetic co-energy $E(i_1, i_2, \ldots)$ of the transformer can be expressed as

$$E(i_1, i_2, \cdots) = \int_{\mathbf{0}}^{\mathbf{i}} \boldsymbol{\psi}(\mathbf{i}) \cdot d\mathbf{i}, \tag{1}$$

where $\mathbf{0}$ is the zero vector.

We seek for the solution of $\mathbf{i}$ that gives an extremum of E under given total primary current I_p and total secondary current I_s. We can easily obtain the solution of $\mathbf{i}$ using Lagrangian multiplier method. For this purpose, we introduce the following function E' defined as

$$\begin{aligned} E'(i_1, i_2, \cdots) = \int_{\mathbf{0}}^{\mathbf{i}} \boldsymbol{\psi}(\mathbf{i}) \cdot d\mathbf{i} - \lambda_p (i_1 + i_2 + \cdots + i_k - I_p) \\ - \lambda_s (i_{k+1} + i_{k+2} + \cdots + i_n - I_s), \end{aligned} \tag{2}$$

where λ_p and λ_s are the Lagrangian multipliers.

The solution requires

$$\frac{\partial E'}{\partial i_1} = \frac{\partial E'}{\partial i_2} = \cdots = \frac{\partial E'}{\partial i_n} = \frac{\partial E'}{\partial \lambda_p} = \frac{\partial E'}{\partial \lambda_s} = 0 . \tag{3}$$

As a result, we obtain

$$\begin{aligned} &\psi_1 = \psi_2 = \cdots = \psi_k = \lambda_p, \\ &\psi_{k+1} = \psi_{k+2} = \cdots = \psi_n = \lambda_s, \\ &i_1 + i_2 + \cdots + i_k = I_p, \\ &i_{k+1} + i_{k+2} + \cdots + i_n = I_s, \end{aligned} \tag{4}$$

The former two equations require that the same voltage should be induced in the parallel-connected windings, because time derivative of $\psi_1, \psi_2, \ldots, \psi_n$ are the voltage induced in the windings. The latter two equations require that the total primary and secondary current are I_p and I_s, respectively. Therefore, the extremum co-energy principle is equivalent to Kirchhoff's current and voltage laws of the transformer windings, thus indicating appropriateness of this principle.

Furthermore, (4) suffices to determine all of $i_1, i_2, \ldots, i_n$ as functions of I_p and I_s, because $\psi_1, \psi_2, \ldots, \psi_n$ are functions of $i_1, i_2, \ldots, i_n$. (Note that $\psi_j = \partial E(i_1, i_2, \ldots)/\partial i_j$ is obtained from (1), where j is an arbitrary number from 1 to n.) This indicates that the extremum co-energy principle suffices to determine the current distribution in the transformer windings.

III. Proposed Analysis Method of Copper Loss

In the proposed copper loss analysis method, we apply the extremum co-energy principle to forward transformers with multiple winding layers to obtain the current distribution in parallel-connected windings. Then, after determining the current in all the winding, we calculate the copper loss.

This section describes this procedure theoretically. In order to simplify the discussion, following assumptions are introduced:

1. The skin depth is smaller than the thickness of each winding layer.
2. The permeability μ of the magnetic core is constant and far larger than the air.

According to assumption 2, the reluctance at the magnetic core is neglected. Furthermore, the magnetic saturation is neglected, for convenience. Hence, the magnetic co-energy is equal to the magnetic energy in this analysis.

Hereafter, we discuss the proposed method based on a generalized transformer model shown in Fig. 2. This model has

multiple winding layers wound on a pair of E cores. According to the Dowell model, we approximate each winding layer as a solid piece of conductor, as shown in Fig. 2(b).

A. Theory

1) Derivation of the AC current distribution: First, we formulate the magnetic co-energy of the transformer. The magnetic co-energy of this transformer is the sum of the co-energy generated by the flux inside the core and that generated by the leakage flux outside the core. The former co-energy is small because the co-energy of a unit volume of the magnetic core is equal to $B^2/2\mu$, where B is the magnetic flux density, and μ is the permeability of the core. Compared with the permeability of the air, μ is assumed to be sufficiently large. Hence, the latter co-energy is the main contributor of the total magnetic co-energy of the transformer.

Next, we estimate the latter co-energy. Because of the skin effect, the AC magnetic field does not penetrate the winding layer. Hence, the latter co-energy is the sum of the co-energy density of the vacant space around the winding layers because the leakage flux occurs outside the winding layers.

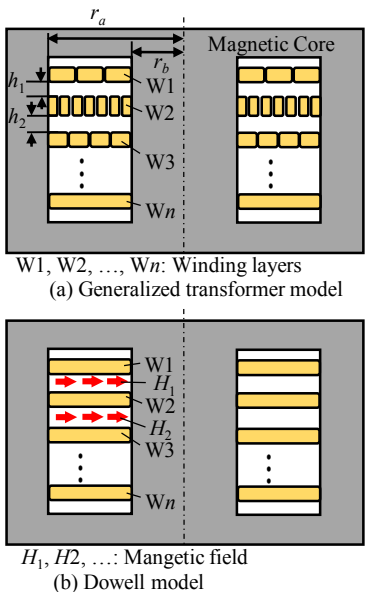

Fig. 2. Generalized forward transformer model and its Dowell model. (Vertical sectional view)

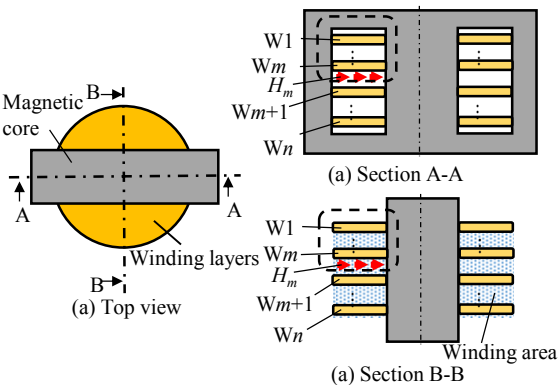

Fig. 3. Definition of vertical sections A-A and B-B in the Dowell model of the forward transformer.

The co-energy density of the vacant space can be estimated as follows. We analyze the magnetic field distribution based on sections A-A and B-B shown in Fig. 3. Note that the magnetic field inside the magnetic core is small because of large permeability of the core. Applying Ampere's law along the closed dashed line shown in section A-A, we can obtain the magnetic field between the windings as

$$H_m = \frac{1}{r_a - r_b}\sum_{j=1}^{m} N_j i'_j, \tag{5}$$

where r_a and r_b are the outer and inner diameter of the winding layers, respectively; m is the index of the winding layer enumerated from the top; H_m is the magnetic field intensity between the winding layers m and m+1; N_j and i'_j is the number of turns and the current of the winding layer j, respectively. (Note that i' is not identical to i in the previous section. The current i' is the current of each winding layer, while i is the current of each winding. By distinguishing a winding layer from a winding, this discussion can consider a winding composed as series-connected multiple winding layers.) The current i'_j takes positive value, if the current passes the section from the bottom to the top. Strictly speaking, the cross-section area of the leakage flux path between winding layers expands near the outer legs. Therefore, the magnetic field between the winding layers is smaller near the outer leg than near the center leg. However, we approximate that the magnetic field is uniform.

Similarly, we apply Ampere's law to the closed dashed line in section B-B. Because the magnetomotive force of the primary and secondary windings cancels each other in the forward transformer, we can neglect the flux circulating outside the winding area. Hence, the most flux in the open space outside the winding area passes through the narrow space between the winding layers.

Because the open space outside the winding area has large cross-section area for magnetic path compared with the flux path between winding layers, we can regard that the flux path in the open space has small reluctance compared with the flux path between winding layers. Therefore, we can approximate that the magnetic field of the open space is negligible and that the magnetic co-energy of the open space is also negligible compared with that of the flux path between the winding layers. As a result, the magnetic field between winding layers is also obtained as in (5).

To summarize, regardless to the section with or without the outer leg, the magnetic field between winding layers is given by (5) and the magnetic co-energy outside the core is mainly contributed by the space between winding layers. Because the total magnetic co-energy E_T is mainly contributed by the co-energy outside the core, we obtain E_T as

$$E_T = \sum_{m=1}^{n-1}\frac{1}{2}\mu_0 H_m^2 h_m \pi\left(r_a^2 - r_b^2\right) = \frac{\pi\mu_0\left(r_a^2 - r_b^2\right)}{2\left(r_a - r_b\right)^2} K_T\left(i'_1, i'_2, \cdots\right), \tag{6}$$

where n is the number of the winding layers, μ_0 is the permeability of the air, h_m is the height of the space between winding layers m and m+1. Function $K_T(i'_1, i'_2, \ldots)$ is defined as

$$K_T = \sum_{m=1}^{n-1} h_m \left(\sum_{j=1}^{m} N_j i'_j \right)^2 . \tag{7}$$

Because E_T is proportional to K_T, the extremum co-energy principle can be interpret as that the current is distributed to give an extremum of K_T under given total primary current I_p and total secondary current I_s. Therefore, current i'_1, i'_2, … can be determined by seeking an extremum of K_T.

We can determine current i'_1, i'_2, …, even if either I_p or I_s is unknown. In this case, we utilize the fact that the total magnetomotive force can be approximated as zero in the forward transformer. Hence, we have

$$\sum_{j=1}^{n} N_j i'_j = 0. \tag{8}$$

This requirement can be employed instead of either the requirement that the total primary current should be I_p or the requirement that total secondary current should be I_s, because (8) can derive the former requirement using I_s as well as the latter using I_p.

2) Derivation of the copper loss: After determining current i'_1, i'_2, … of the winding layers, we can estimate the copper loss. Because of assumption 1, high frequency AC current flows at the surface of the conductor; and amount of the AC current crossing unit length of the surface is equal to the AC magnetic field at the surface. The reason is demonstrated in the appendix. Noting that each winding layer is regarded as a solid piece of conductor in the Dowell model, we can define i''_{m_t} and i''_{m_b} as the total surface current flowing at the top and bottom surfaces of winding layer m, respectively. Hence, $i'_m = i''_{m\_t} + i''_{m\_b}$. Because the bottom surface of winding layer m and the top surface of winding layer m+1 share the same magnetic field of the space between the winding layer m and m+1, we have $i''_{m\_b} = i''_{m+1\_t} = H_m(r_a - r_b)$.

According to the electromagnetism, the copper loss generated in the unit area of the surface of the conductor is equal to the Joule loss when the surface current flows uniformly within the skin depth δ. The reason is demonstrated in the appendix. Hence, the copper loss p_{m_b} of the bottom surface of winding layer m and the copper loss p_{m+1_t} of the top surface of winding layer m+1 is given as

$$p_{m\_b} = p_{m+1\_t} = \frac{\rho\pi(r_a + r_b)}{(r_a - r_b)\delta} i''^2_{m\_b} = \frac{\rho\pi(r_a + r_b)}{(r_a - r_b)\delta} H_m^2 (r_a - r_b)^2 . \tag{9}$$

where ρ is the resistivity of the copper. Because of (8), the magnetic field at the bottom surface of winding layer n is zero. Therefore, $p_{n\_b} = 0$. Similarly, because the magnetic field at the top surface of winding layer 1 is zero, $p_{1\_t} = 0$

An actual winding layer, however, is not a solid conductor. Therefore, the copper does not entirely cover the width of the winding layer. If we introduce the porosity factor η_m defined as the occupation ratio of the copper in the width of winding layer m, we can estimate the copper loss at the surface of the actual winding layers. As a result, we have

$$\begin{aligned} p_{m\_b} &= \frac{\rho\pi(r_a + r_b)}{\eta_m (r_a - r_b)\delta} i''^2_{m\_b} = \frac{\rho\pi\left(r_a^2 - r_b^2\right)}{\eta_m \delta} H_m^2, \\ p_{m+1\_t} &= \frac{\rho\pi(r_a + r_b)}{\eta_{m+1} (r_a - r_b)\delta} i''^2_{m\_t} = \frac{\rho\pi\left(r_a^2 - r_b^2\right)}{\eta_{m+1} \delta} H_m^2. \end{aligned} \tag{10}$$

Finally, we can estimate the total copper loss P in the transformer using (5), noting that $p_{n\_b} = p_{1\_t} = 0$.

$$\begin{aligned} P &= p_{1\_t} + \sum_{m=1}^{n-1} \left(p_{m\_b} + p_{m+1\_t} \right) + p_{n\_b} \\ &= \frac{\rho\pi(r_a + r_b)}{\delta(r_a - r_b)} \sum_{m=1}^{n-1} \left\{ \left(\frac{1}{\eta_m} + \frac{1}{\eta_{m+1}} \right) \left(\sum_{j=1}^{m} N_j i'_j \right)^2 \right\}. \end{aligned} \tag{11}$$

B. Example 1

This subsection presents a simple example of the copper loss analysis of the transformer shown in Fig. 4. This transformer has three winding layers wound on EI cores: an N-turn winding layer (W1) of the primary winding, and two one-turn winding layers (W2 and W3) of the secondary windings. These secondary windings are connected in parallel at the secondary terminal. We denote the current in W2 and W3 as i'_2 and i'_3, respectively. Then, K_T is formulated according to (7):

$$K_T = h_1 N^2 I_p^2 + h_2 \left(N I_p - i'_2 \right)^2, \tag{12}$$

where h_1 are the height of the space between W1 and W2, and h_2 is that between W2 and W3.

Obviously, K_T is at an extremum, when $i'_2 = NI_p$. This indicates that $i'_3 = 0$ because $I_s = NI_p$ according to (8). Therefore, all of the secondary current must flow in W2.

Consequently, we obtain the total copper loss P_1:

$$P_1 = \frac{\rho\pi(r_a + r_b)}{\delta(r_a - r_b)} \left(\frac{1}{\eta_1} + 1 \right) N^2 I_p^2, \tag{13}$$

where η_1 is the porosity factor of W1. The porosity factor of W2 and W3 is assumed to be 1.

C. Example 2

Next, another simple example is presented based on the transformer shown in Fig. 5. This transformer has the same winding layers W1, W2, and W3, similarly as in Fig. 4. However, W2 and W3 are disposed to sandwich W1. In this case, K_T is formulated as

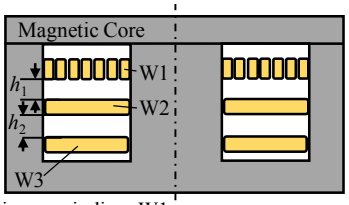

Primary winding: W1
Secondary winding: W2, W3 (connected in parallel)

Fig. 4. Transformer structure of example 1. (Vertical sectional view)

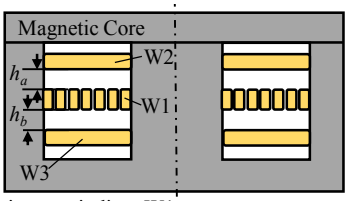

Primary winding: W1
Secondary winding: W2, W3 (connected in parallel)

Fig. 5. Transformer structure of example 2. (Vertical sectional view)

$$K_T = h_a i_2'^2 + h_b \left(NI_p - i_2'\right)^2 = \left(h_a + h_b\right)\left(i_2' - \frac{h_b}{h_a + h_b} NI_p\right)^2 + \frac{h_a h_b}{h_a + h_b} N^2 I_p^2, \quad (14)$$

where h_a are the height of the space between W2 and W1, and h_b is that between W1 and W3.

Therefore, K_T is at an extremum, when $i'_2=h_b/(h_a+h_b)NI_p$. The current i'_3 is determined as $i'_3=h_a/(h_a+h_b)NI_p$ because $I_s=NI_p$ according to (8). Hence, the secondary current is divided into i'_2 and i'_3 in the ratio $h_b : h_a$.

Consequently, we obtain the total copper loss P_2 as

$$P_2 = \frac{\rho\pi\left(r_a + r_b\right)}{\delta\left(r_a - r_b\right)}\left(\frac{1}{\eta_1} + 1\right)\frac{h_a^2 + h_b^2}{\left(h_a + h_b\right)^2} N^2 I_p^2, \quad (15)$$

This result indicates that P_2 is always smaller than P_1. Furthermore, the extremum value of P_2 is half of P_1, which is achieved when $h_a=h_b$. Therefore, Fig. 5 can reduce the copper loss into half of that in Fig. 4, if we design the same height for h_a and h_b.

IV. Experiment

Experiments were carried out to verify the proposed method of copper loss analysis. In this experiment, the current in parallel-connected windings and the parasitic AC resistance caused by the copper loss are measured in the transformers with the same structure as Fig. 4 and Fig. 5. Then, the results are compared with the theory discussed in the previous section.

The experimental transformers are shown in Fig. 6. The transformers are composed of the EI cores without any gaps in the magnetic path. The primary winding forms a winding layer of six turns (W1); and the two parallel-connected secondary windings form two winding layers of one turn (W2 and W3).

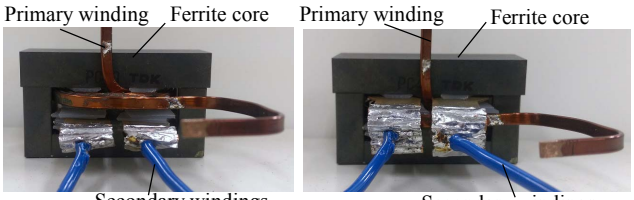

(a) Example 1 (b) Example 2

Fig. 6. Photographs of the experimental transformers for examples 1 and 2.

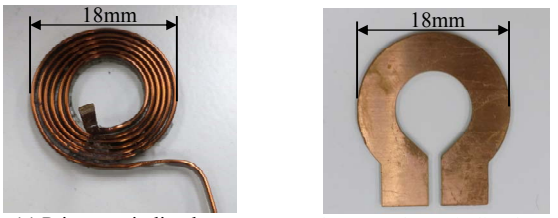

(a) Primary winding layer (b) Secondary winding layer

Fig. 7. Photographs of the primary and secondary winding layers.

TABLE I. Specifications of Experimental Transformers

Parameter		Value
Outer diameter of winding layers	r_a	18mm
Inner diameter of winding layers	r_b	9.0mm
Number of turns (primary winding)	N	6T
Thickness of primary winding		3.0mm
Thickness of secondary winding		0.5mm
Porosity factor of primary winding	η_1	63%
Porosity factor of secondary winding		100%

Photographs of the winding layers are shown in Fig. 7. Specifications are presented in Table 1.

A. Current in Parallel-Connected Winding

First, we evaluated the current in the two winding layers W2 and W3 to verify the extremum co-energy principle. The secondary winding of the experimental transformers was connected to the load with various resistance; and the primary winding was supplied with AC current of 200mArms, 100kHz. The skin depth of copper is estimated as 0.21mm at 100kHz.

Fig. 8 shows the results of example 1, i.e. Fig. 6(a). Height h_1 and h_2 of the space between the winding layers were both set at 3.2mm. The results revealed that almost all the secondary current flowed in W2 regardless to the load resistance, which is consistent with the theory.

Fig. 9 shows the results of example 2, i.e. Fig. 6(b). Height h_a and h_b were set at various values so that we can evaluate the dependency of the current on the ratio h_b:h_a. The results revealed that the current ratio of W2 and W3 was close to the ratio h_b:h_a regardless to the load resistance, which is also consistent with the theory.

B. Parasitic AC Resistance Caused by Copper Loss

Next, we evaluated the copper loss of the experimental transformers. For this purpose, the secondary windings were

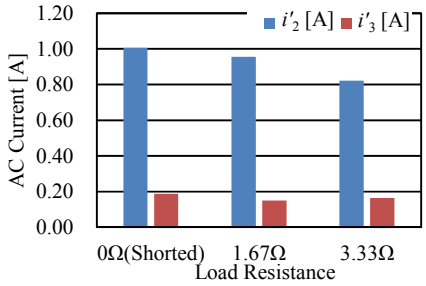

Fig. 8. AC current in two secondary winding layers of Example 1.

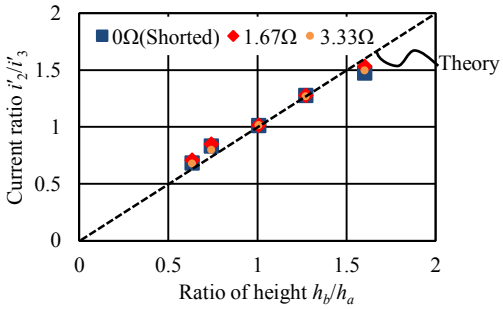

Fig. 9. Ratio of AC current in two secondary winding layers of Example 2.

short-circuited; and the primary winding was supplied with AC current of 1Arms, 100kHz. Then, we measured the AC resistance of the primary winding and compared the result with the theory.

Fig. 10 shows the results for examples 1 and 2, respectively. Height h_1, h_2, h_a, and h_b were all set at 3.2mm. These results agreed well with the theory within an error of 8%, indicating the appropriateness of the theory.

V. Conclusions

This paper proposed a copper loss analysis method applicable to high frequency forward transformers with parallel-connected windings. The proposed method employs the Dowell model in combination with a novel insight that the AC current is distributed in parallel-connected windings to give an extremum of the magnetic co-energy of the transformer. This insight can determine the current distribution in the parallel-connected windings, thus enabling the Dowell model to be applied to the transformers with parallel-connected windings.

Along with the theory of the proposed method, this paper also presented two simple examples of analysis. These analysis results were successfully verified by the experiment, supporting appropriateness of the proposed method.

Appendix

This appendix demonstrates that the surface current of the conductor per unit length is equal to the surface magnetic field. Furthermore, this appendix demonstrates that the copper loss generated in the unit area of the surface of the conductor is equal to the Joule loss when the surface current flows uniformly within the skin depth.

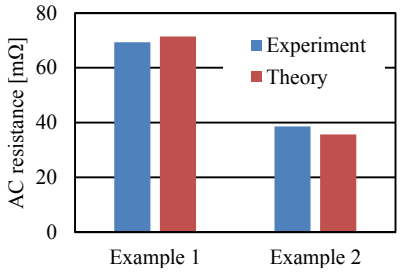

Fig. 10. Experimental results and theoretical prediction of the AC resistance of the primary current.

We assume that the conductor have far larger thickness than the skin depth. Therefore, we approximate that the conductor has infinitely large depth, because we focus on the surface current. Furthermore, we assume uniform magnetic field along the surface of the conductor. We take the x-axis and the z-axis in the direction of the surface AC magnetic field and the depth, respectively, as shown in Fig. 11. The y-axis is taken in perpendicular to the x-axis and the y-axis.

According to Maxwell equations, we have following relations inside the conductor. (We assume constant permeability μ.)

$$\nabla\times\mathbf{E}+\mu\frac{d\mathbf{H}}{dt}=0,\quad \nabla\times\mathbf{H}-\frac{d\mathbf{D}}{dt}=\mathbf{j}\quad \nabla\cdot\mathbf{H}=0. \tag{16}$$

where **E**, **H**, **D**, and **j** are the electric field, magnetic field, electric flux density, and current vector. We neglect **D** inside the conductor. Furthermore, we assume $\mathbf{E}=\rho\mathbf{j}$, where ρ is the resistivity of the conductor. Then, (16) is reduced to

$$\begin{aligned}&\nabla\times(\nabla\times\mathbf{H})=\nabla(\nabla\cdot\mathbf{H})-\Delta\mathbf{H}=-\frac{\mu}{\rho}\frac{d\mathbf{H}}{dt}.\\&\therefore\Delta\mathbf{H}=\frac{\mu}{\rho}\frac{d\mathbf{H}}{dt}\end{aligned} \tag{17}$$

Partial derivative in the x and y direction must vanish because uniform magnetic field is assumed. Furthermore, the magnetic field in the y and z directions must vanish because zero field in the y and z directions suffices (17) as well as the boundary condition at the surface. Therefore, the magnetic field inside the conductor is in the x direction; and, the current vector is in the y direction.

Let H_0 be the surface magnetic field given as

$$H_0=H_{0\_amp}\exp(j\omega t), \tag{18}$$

where H_{0_amp} and ω are the amplitude and the angular velocity of the surface magnetic field. If we denote the magnitude of **H** and **j** inside the conductor as $H(z)$ and $j(z)$, respectively, (17) is reduced to

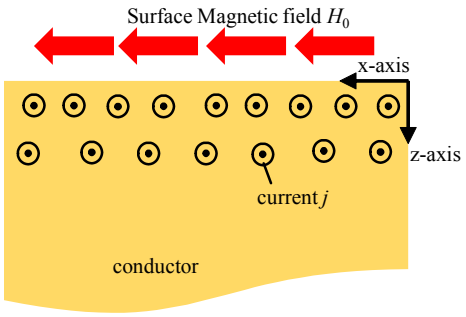

Fig. 11. Definition of the system under consideration.

$$\frac{\partial^2 H}{\partial z^2} = j\omega\frac{\mu}{\rho}H. \tag{19}$$

Then, solution of H and j is obtained as

$$H = H_0 \exp\left(-\frac{1+j}{\delta}z\right), \quad j = -\frac{1+j}{\delta}H_0 \exp\left(-\frac{1+j}{\delta}z\right), \tag{20}$$

where δ is the skin depth defined as

$$\delta = \sqrt{\frac{2\rho}{\omega\mu}}. \tag{21}$$

The total surface current I per unit length of the surface can be obtained by integrating j in the z direction:

$$I = \int_0^\infty j dz = H_0. \tag{22}$$

Equation (22) indicates that the surface current of the conductor per unit length is equal to the surface magnetic field.

Furthermore, the total copper loss P per unit area of the surface can be obtained as

$$P = \int_0^\infty \rho j_{\text{rms}}^2 dz = \frac{\rho H_{0\_\text{amp}}^2}{2\delta} = \frac{\rho}{\delta} I_{\text{rms}}^2, \tag{23}$$

where j_{rms} and I_{rms} are the root-mean-square value of j and I, respectively. Therefore, the copper loss in the unit area of the surface of the conductor is equal to the Joule loss when the surface current flows uniformly within the skin depth.

ACKNOWLEDGMENT

This work was supported by Electric Technology Research Foundation of Chugoku.

REFERENCES

[1] W. Chen, Y. Yan, Y. Hu, and Q. Lu, "Model and design of PCB parallel winding for planar transformer," IEEE Trans. Magn., vol. 39, no. 5, pp. 3202–3204, Sept. 2003.

[2] D. Fu, F. C. Lee, and S. Wang, "Investigation on transformer design of high frequency high efficiency DC-DC converters," in Proc. IEEE Appl. Power Electron. Conf. Expo. (APEC2010), Palm Springs, CA, USA, pp. 940–947, Feb. 2010.

[3] X. Margueron, A. Besri, Y. Lembeye, and J.-P. Keradec, "Current sharing between parallel turns of a planar transfomer: prediction and improvement using a circuit simulation software," IEEE Trans. Ind. Appl., vol. 46, no. 3, pp. 1064–1070, May/Jun. 2010.

[4] R. Asensi, R. Prieto, and J. A. Cobos, "Automatized connection of the layers of planar transformers with parallel windings to improe the component behavior," in Proc. IEEE Applied Power Electron. Conf. Expo. (APEC2012), Orlando, FL, USA, pp. 1778–1782, Feb. 2012.

[5] V. Nabaei, S. A. Mousavi, K. Miralikhani, and H. Mohseni, "Balancing current distribution in parallel windings of furnace transformers using generic algorithm," IEEE Trans. Magn., vol. 46, no. 2, pp. 626–629, Feb. 2010.

[6] M. Chen, M. Araghchini, K. K. Afridi, J. H. Lang, C. R. Sullivan, and D. J. Perreault, "A systematic approach to modeling impedances and current distribution in planar magnetics," IEEE Trans. Power Electron., vol. 31, no. 1, pp. 560–580, Jan. 2016.

[7] J.-P. Vandelac and P. D. Ziogas, "A novel approach for minimizing high-frequency transformer copper loss," IEEE Trans. Power Electron., vol. 3, no. 3, pp. 266–277, Jul. 1988.

[8] J. A. Ferreira, "Appropriate modelling of conductive losses in the design of magnetic components," in Proc. IEEE Power Electron. Specialist Conf. (PESC1990), San Antonio, TX, USA, pp. 780–785, Jun. 1990.

[9] F. Robert and P. Mathys, "Ohmic losses calculation in SMPS transformers: numerical study of Dowell's approach accuracy," IEEE Trans. Magn., vol. 34, no. 4, pp. 1255–1257, Jul. 1998.

[10] W. G. Hurley, E. Gath, and J. G. Breslin, "Optimizing the AC resistance of multilayer transformer windings with arbitrary current waveforms," IEEE Power Electron., vol. 15, no. 2, pp. 369–376, Mar. 2000.

[11] J. T. Strydom and J. D. van Wyk, "Improved loss determination for planar integrated power passive modules," in Proc. IEEE Appl. Power Electron. Conf. Expo. (APEC2002), Dallas, TX, USA, vol. 1, pp. 332–338, Mar. 2002.

[12] R. Pittini, Z. Zhang, M. A. E. Andersen, "High current planar transformer for very high efficiency isolated boost DC-DC converters," in Proc. IEEE Intl. Power Elecron. Conf. (IPEC2014), Hiroshima, Japan, pp. 3905–3912, May 2014.

[13] M. A. Bahmani, T. Thiringer, and H. Ortega, "An accurate pseudoempirical model of winding loss calculation in HF foil and round conductors in switchmode magnetics," IEEE Trans. Power Electron., vol. 29, no. 8, pp. 4231–4246, Aug. 2014.

[14] J. M. Lopera, M. J. Prieto, J. Diaz, and J. Garcia, "A mathematical expression to determine copper losses in switch-mode power supplies transformers including geometry and frequency effects," IEEE Trans. Power Electron., vol. 30, no. 4, pp. 2219–2231, April 2015.

[15] R. Krishnan, Switched reluctance motor drives, Boca Raton, FL, USA: CRC Press, 2000, pp. 3–7.

[16] T. J. E. Miller, Electronic control of switched reluctance machines, Oxford, U. K.: Newns, 2001, pp. 43–45.